axioms

MDPI

Article

On the Wave Structures to the (3+1)-Dimensional Boiti–Leon–Manna–Pempinelli Equation in Incompressible Fluid

Yan-Nan Chen and Kang-Jia Wang *

School of Physics and Electronic Information Engineering, Henan Polytechnic University, Jiaozuo 454003, China
* Correspondence: konka05@163.com

Abstract: In the present study, two effective methods, the Exp-function method and He's frequency formulation, are employed to investigate the dynamic behaviors of the (3+1)-dimensional Boiti–Leon–Manna–Pempinelli equation, which is used widely to describe the incompressible fluid. A variety of the wave structures, including the dark wave, bright-dark wave and periodic wave solutions, are successfully constructed. Compared with the results attained by the methods, the obtained solutions are all new and have not been presented in the other literature. The diverse wave structures of the solutions are presented through numerical results in the form of three-dimensional plots and two-dimensional curves. It reveals that the proposed methods are powerful and straightforward, which are expected to be helpful for the study of travelling-wave theory in fluid.

Keywords: Exp-function method; He's frequency formulation; solitary solutions; periodic wave solution

MSC: 35Q35; 35Q51

check for updates

Citation: Chen, Y.-N.; Wang, K.-J. On the Wave Structures to the (3+1)-Dimensional Boiti–Leon–Manna–Pempinelli Equation in Incompressible Fluid. *Axioms* **2023**, *12*, 519. https://doi.org/10.3390/axioms12060519

Academic Editors: Evangelos Melas and Simeon Reich

Received: 24 April 2023
Revised: 15 May 2023
Accepted: 23 May 2023
Published: 25 May 2023

1. Introduction

Exploration of the exact solutions of the partial differential equations (PDEs) has obtained wide attention from scientists and mathematicians. Until now, some effective approaches thus far are: the auxiliary equation mapping method [1,2], Wang's Bäcklund transformation based method [3,4], the modified extended direct algebraic method [5,6], Sardar subequation method [7,8], variational method [9,10], trial equation method [11,12], logarithmic transformation [13] and so on. As is common knowledge, the fluid, as a phase of matter including liquid, gas and plasma, is considered to be one of the most common substances in nature. Significant research on fluids has provided an important guide for the design of related industries. Additionally, there are many famous partial–differential equations available to model fluid characteristics. In this paper, we consider the famous (3+1)-dimensional Boiti–Leon–Manna–Pempinelli (BLMP) equation, which is provided by [14,15]:

$$\psi_{yt} + \psi_{zt} + \psi_{xxxy} + \psi_{xxxz} - 3\psi_x(\psi_{xy} + \psi_{xz}) - 3\psi_{xx}(\psi_y + \psi_z) = 0 \tag{1}$$

where $\psi = \psi(x, y, z, t)$ is a well-known function that is used widely in the liquid engendering and incompressible liquid. Additionally, many scholars have made outstanding contributions to the solution of Equation (1). MelikeKaplan used the transformed rational function to construct different types of analytical solutions [16]. In [17], Mohamed R. Ali et al, obtained the lump solutions and mixed solution involving lump waves and solitons by the bilinear method and symbolic computation. Tang et al. found the periodic wave solutions for Equation (1) via the extended homoclinic test approach [18]. Additionally, the double-periodic soliton solutions are constructed by Liu in [19]. The sine Gordon expansion method and the extended tanh function method are used to seek the new soliton solutions in [20]. Mohammad Najafi et al. studied the problem via the semi-inverse method [21]. The Hirota's bilinear algorithm is applied to seek the lump solutions by Ahmad M.Alenezi in [22]. Considering the importance of Equation (1) in the field of fluids, and being encouraged by recent research results, we aim to construct abundant exact solutions of Equation (1) by the Exp-function method (EFM) and He's frequency formulation (HFF). The structure of this paper is as follows. In Section 2, we will provide a brief introduction to the EFM and HFF. In Section 3, the EFM and HFF are used to find the exact solutions and the behaviors of the different solutions are presented by the three-dimensional and two-dimensional contours. The physical explanation of the different solutions are provided in Section 4. The conclusion is presented in Section 5.

2. The Two Methods

Considering the general nonlinear FDEs as:

$$F(u, u_x, u_y, u_z, u_t, \ldots) = 0 \tag{2}$$

Introducing the following transformation:

$$u(x, y, z, t) = U(\xi),\ \xi = \omega x + my + kz + vt \tag{3}$$

where ω, m, k, v are all non-zero constant. using Equation (3), the nonlinear PDE of Equation (2) can be reduced into the ODE as:

$$F(U, U_\xi, U_{\xi\xi}, U_{\xi\xi\xi}, \ldots) = 0 \tag{4}$$

2.1. The EFM

The EFM is a powerful tool to construct the abundant traveling wave solutions of the studied equation. In this section, we will provide a brief introduction to the EFM [23–27]. Its primary steps are presented as follows:

Assuming the solution of Equation (4) with the form as:

$$U(\xi) = \frac{\sum\limits_{i=-p}^{u} a_i \exp(i\xi)}{\sum\limits_{j=-g}^{s} b_j \exp(j\xi)} \tag{5}$$

where u, p, s, g are positive integers that can be determined later, a_i, b_j are unknown constants.

Taking Equation (5) into Equation (4) and balancing the linear term of highest and lowest orders, respectively, we can determine the u, p, s, g.

Then, substituting the obtained results into Equation (4), setting the coefficients of $\exp(i\xi)$ to be zero, we can determine the coefficients a_i and b_j. With this, we can obtain the exact solutions of Equation (2) via Equation (3).

2.2. The HFF

The HFF [28–30], which was first proposed by Chinese mathematician Ji-Huan He, is a powerful tool to seek the periodic solution.

Considering Equation (4) with the form as:

$$U'' + f(U) = 0 \tag{6}$$

In Equation (6), $f(U)$ is a function of U. Here, the periodic solution of Equation (6) can be assumed as:

$$U(\xi) = M\cos(\Omega\xi),\ \Omega > 0 \tag{7}$$

where Ω represents angular frequency. In the view of He's frequency formulation [31,32], the amplitude–frequency relationship of Equation (7) can be determined via one step, which is:

$$\Omega^2 = \left.\frac{df(U)}{dU}\right|_{U=\frac{M}{2}} \tag{8}$$

With this, we can obtain the periodic wave solution of Equation (1).

3. Applications

In order to obtain the abundant solutions, the following transformation is introduced:

$$\psi(x,y,z,t) = \Psi(\xi),\ \xi = \omega x + my + kz + vt + \xi_0 \tag{9}$$

In Equation (9), ω, m, k and v are non-zero real numbers, and there is $m + k \neq 0$. With the help of Equation (9), Equation (1) becomes an ordinary differential equation, which is:

$$(m+k)v\Psi'' + \omega^3(m+k)\Psi^{(4)} - 6\omega^2(m+k)\Psi'\Psi'' = 0 \tag{10}$$

Additionally, there are $\Psi' = \frac{d\Psi}{d\xi}$, $\Psi = \frac{d^2\Psi}{d\xi^2}$ and $\Psi^{(4)} = \frac{d^4\Psi}{d\xi^4}$.

Integrating Equation (10) once, with respect to ξ, and setting the integral constant to be zero, yields:

$$(m+k)v\Psi' + \omega^3(m+k)\Psi^{(3)} - 3\omega^2(m+k)\left(\Psi'\right)^2 = 0 \tag{11}$$

which is:

$$v\Psi' + \omega^3\Psi^{(3)} - 3\omega^2\left(\Psi'\right)^2 = 0 \tag{12}$$

3.1. Application of the EFM

Based on the EFM, we assume the solution of Equation (12) with the form as:

$$\Psi(\xi) = \frac{\sum\limits_{i=-u}^{c} a_i \exp(i\xi)}{\sum\limits_{j=-s}^{g} b_j \exp(j\xi)} \tag{13}$$

which can be expressed as:

$$\Psi(\xi) = \frac{a_c \exp(c\xi) + \ldots + a_{-u}\exp(-u\xi)}{b_g \exp(g\xi) + \ldots + b_{-s}\exp(-s\xi)} \tag{14}$$

Putting Equation (14) into Equation (12) and balancing the linear term of highest order $\Psi^{(3)}$ and $\left(\Psi'\right)^2$ in Equation (12) with the highest order nonlinear term, we obtain:

$$\Psi^{(3)} = \frac{p_1 \exp[(3g+c)\xi] + \ldots}{p_2 \exp(4g\xi) + \ldots} \tag{15}$$

$$\left(\Psi'\right)^2 = \frac{p_3 \exp[(2g+2c)\xi] + \ldots}{p_4 \exp(4g\xi) + \ldots} \tag{16}$$

By balancing the highest order of Exp-function in Equations (15) and (16), it yields:

$$3g + c = 2g + 2c \tag{17}$$

which leads to:

$$g = c \tag{18}$$

In the same way, we balance the linear term of lowest order in Equation (12), there is:

$$\Psi^{(3)} = \frac{\ldots + q_1 \exp[-(3s+u)\xi]}{\ldots + q_2 \exp(-4s\xi)} \tag{19}$$

$$\left(\Psi'\right)^2 = \frac{\ldots + q_3 \exp[-(2s+2u)\xi]}{\ldots + q_4 \exp(-4s\xi)} \tag{20}$$

Balancing the lowest order of Exp-function in Equations (19) and (20), there is:

$$-3s - u = -2s - 2u \tag{21}$$

which results in:

$$u = s \tag{22}$$

For simplicity, we set $g = c = 1$, $u = s = 1$ and $b_1 = 1$, Equation (14) can be written as:

$$\Psi(\xi) = \frac{a_1 \exp(\xi) + a_0 + a_{-1}\exp(-\xi)}{\exp(\xi) + b_0 + b_{-1}\exp(-\xi)} \tag{23}$$

Taking Equation (23) into Equation (12), we can obtain the following form:

$$\frac{\begin{bmatrix} M_3 \exp(3\xi) + M_2 \exp(2\xi) + M_1 \exp(\xi) + M_0 + M_{-1}\exp(-\xi) + M_{-2}\exp(-2\xi) \\ +M_{-3}\exp(-3\xi) \end{bmatrix}}{[\exp(\xi) + b_0 + b_{-1}\exp(-\xi)]^4} = 0 \tag{24}$$

where

$$\begin{aligned}
M_3 = \quad & -\omega^3 a_0 - v a_0 + \omega^3 a_1 b_0 + v a_1 b_0 \\
M_2 = \quad & -8\omega^3 a_{-1} - 2v a_{-1} - 3\omega^2 a_0^2 + 8\omega^3 a_1 b_{-1} + 2v a_1 b_{-1} + 4\omega^3 a_0 b_0 - 2v a_0 b_0 + 6\omega^2 a_0 a_1 b_0 \\
& -4\omega^3 a_1 b_0^2 + 2v a_1 b_0^2 - 3\omega^2 a_1^2 b_0^2 \\
M_1 = \quad & -12\omega^2 a_{-1} a_0 + 23\omega^3 a_0 b_{-1} - v a_0 b_{-1} + 12\omega^2 a_0 a_1 b_{-1} - 5\omega^3 a_{-1} b_0 - 5v a_{-1} b_0 + 12\omega^2 a_{-1} a_1 b_0 \\
& -18\omega^3 a_1 b_{-1} b_0 + 6v a_1 b_0 b_{-1} - 12\omega^2 a_1^2 b_{-1} b_0 - \omega^3 a_0 b_0^2 - v a_0 b_0^2 + \omega^3 a_1 b_0^3 + v a_1 b_0^3 \\
M_0 = \quad & -12\omega^2 a_{-1}^2 + 32\omega^3 a_{-1} b_{-1} - 4v a_{-1} b_{-1} + 6\omega^2 a_0^2 b_{-1} + 24\omega^2 a_{-1} a_1 b_{-1} - 32\omega^3 a_1 b_{-1}^2 + 4v a_{-1} b_{-1}^2 \\
& -12\omega^2 a_1^2 b_{-1}^2 - 6\omega^2 a_{-1} a_0 b_0 - 6\omega^2 a_0 a_1 b_0 b_{-1} + 4\omega^3 a_{-1} b_0^2 - 4v a_{-1} b_0^2 \\
& +6\omega^2 a_{-1} a_1 b_0^2 + 4\omega^3 a_1 b_{-1} b_0^2 + 4v a_1 b_{-1} b_0^2 \\
M_{-1} = \quad & 12\omega^2 a_{-1} a_0 b_{-1} - 23\omega^3 a_0 b_{-1}^2 + v a_0 b_{-1}^2 - 12\omega^2 a_0 a_1 b_{-1}^2 - 12\omega^2 a_{-1}^2 b_0 + 18\omega^3 a_{-1} b_0 b_{-1} - 6v a_{-1} b_{-1} b_0 \\
& -12\omega^2 a_{-1} a_1 b_{-1} b_0 + 5\omega^3 a_1 b_0 b_{-1}^2 + 5v a_1 b_{-1}^2 b_0 + \omega^3 a_0 b_{-1} b_0^2 + v a_0 b_{-1} b_0^2 - \omega^3 a_1 b_0^3 - v a_{-1} b_0^3 \\
M_{-2} = \quad & -8\omega^3 a_{-1} b_{-1}^2 - 2v a_{-1} b_{-1}^2 - 3\omega^2 a_0^2 b_{-1}^2 + 8\omega^3 a_1 b_{-1}^3 + 2v a_1 b_{-1}^3 + 6\omega^2 a_{-1} a_0 b_{-1} b_0 - 4\omega^3 a_0 b_{-1}^2 b_0 \\
& +2v a_0 b_{-1}^2 b_0 - 3\omega^2 a_{-1}^2 b_0^2 + 4\omega^3 a_{-1} b_{-1} b_0^2 - 2v a_{-1} b_{-1} b_0^2 \\
M_{-3} = \quad & \omega^3 a_0 b_{-1}^3 + v a_0 b_{-1}^3 - \omega^3 a_{-1} b_{-1}^2 b_0 - v a_{-1} b_{-1}^2 b_0
\end{aligned}$$

Letting the coefficients of $\exp(i\xi)$ to be zero, we obtain:

$$\begin{cases} M_3 = 0, M_2 = 0, M_1 = 0 \\ M_0 = 0 \\ M_{-1} = 0, M_{-2} = 0, M_{-3} = 0 \end{cases}$$

Solving the above systems, we obtain the following three families:

Family 1

Set 1: $a_1 = a_1$, $a_0 = \omega b_0 + a_1 b_0 + \sqrt{\omega^2 b_0^2 - 4\omega^2 b_{-1}}$, $a_{-1} = (2\omega + a_1) b_{-1}$, $b_0 = b_0$, $b_{-1} = b_{-1}$, $v = -\omega^3$, $\omega = \omega$.

Therefore, we can get the first exact traveling wave solution (dark-wave solution Form 1) as:

$$\psi_1(x,y,t,z)=\frac{\left[\begin{array}{c}a_1\exp\left(\omega x+my+kz-\omega^3 t+\xi_0\right)+\omega b_0+a_1 b_0+\sqrt{\omega^2 b_0^2-4\omega^2 b_{-1}}\\+(2\omega+a_1)b_{-1}\exp\left(-\omega x-my-kz+\omega^3 t-\xi_0\right)\end{array}\right]}{\left[\begin{array}{c}\exp\left(\omega x+my+kz-\omega^3 t+\xi_0\right)+b_0\\+b_{-1}\exp\left(-\omega x-my-kz+\omega^3 t-\xi_0\right)\end{array}\right]} \tag{25}$$

Here, a_1, b_0, b_{-1} and ω are free parameters. If we select $m=1$, $k=1$, $\xi_0=0$, the behavior of solution $\psi_1(x,y,z,t)$ is plotted in Figure 1.

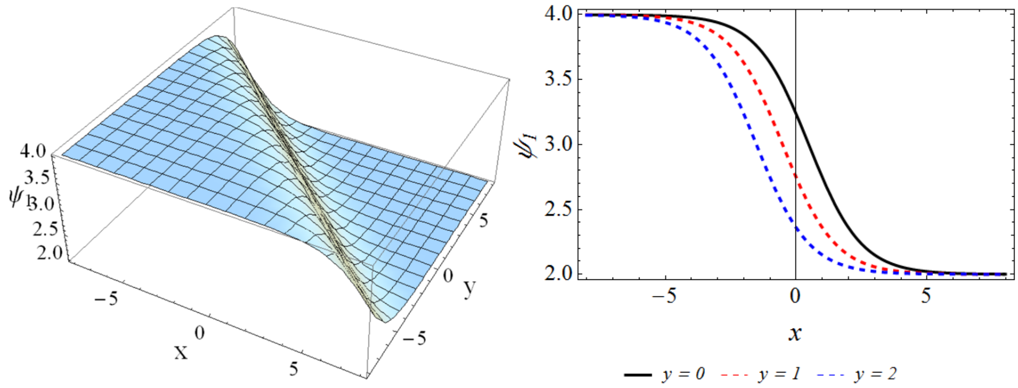

Figure 1. The 3D plot and 2D curve of the solution $\psi_1(x,y,z,t)$ for $\omega=1, a_1=2, b_0=1, b_{-1}=-1$ when $z=1, t=1$.

Set 2: $a_1=a_1$, $a_0=\omega b_0+a_1 b_0-\sqrt{\omega^2 b_0^2-4\omega^2 b_{-1}}$, $a_{-1}=(2\omega+a_1)b_{-1}$, $b_0=b_0$, $b_{-1}=b_{-1}$, $v=-\omega^3$, $\omega=\omega$.

Furthermore, we can obtain the second exact traveling solution (bright-dark wave solution) as:

$$\psi_2(x,y,t,z)=\frac{\left[\begin{array}{c}a_1\exp\left(\omega x+my+kz-\omega^3 t+\xi_0\right)+\omega b_0+a_1 b_0-\sqrt{\omega^2 b_0^2-4\omega^2 b_{-1}}\\+(2\omega+a_1)b_{-1}\exp\left(-\omega x-my-kz+\omega^3 t-\xi_0\right)\end{array}\right]}{\left[\begin{array}{c}\exp\left(\omega x+my+kz-\omega^3 t+\xi_0\right)+b_0\\+b_{-1}\exp\left(-\omega x-my-kz+\omega^3 t-\xi_0\right)\end{array}\right]} \tag{26}$$

where a_1, b_0, b_{-1} and ω are free parameters. By selecting $m=1$, $k=1$, $\xi_0=0$, the propagation of solution $\psi_1(x,y,z,t)$ is described in Figure 2.

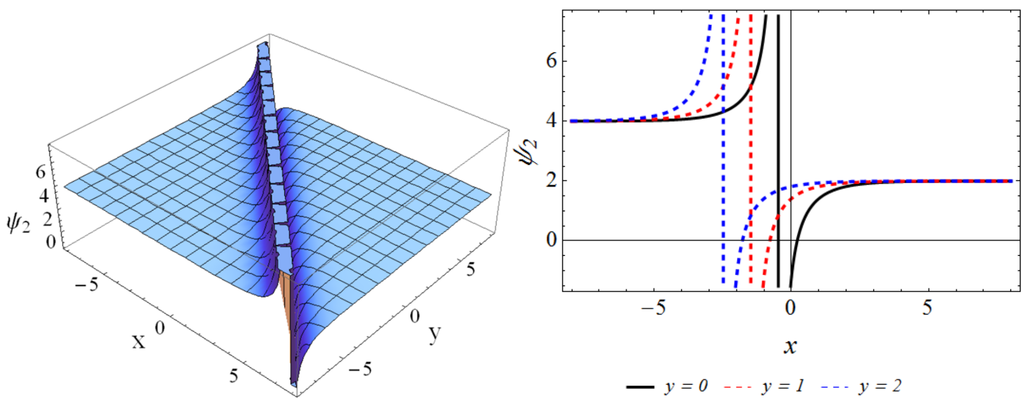

Figure 2. The 3D plot and 2D curve of the solution $\psi_2(x,y,z,t)$ for $\omega=1, a_1=2, b_0=1, b_{-1}=-1$ when $z=1, t=1$.

Family 2

Set 3: $a_1 = \frac{a_0 b_0 - \omega b_0^2 - \sqrt{\omega^2 b_0^4 - 4\omega^2 b_{-1} b_0^2}}{b_0^2}$, $a_0 = a_0$, $a_{-1} = \omega b_{-1} + \frac{a_0 b_{-1}}{b_0} - \frac{\omega b_{-1}\sqrt{-\omega^2 b_0^2 (4b_{-1} - b_0^2)}}{b_0^2}$, $b_0 = b_0$, $b_{-1} = b_{-1}$, $v = -\omega^3$, $\omega = \omega$.

Next, we can obtain the third exact traveling wave solution (dark-solitary wave solution Form 2):

$$\psi_3(x, y, t, z) = \frac{\left[\begin{array}{c} \frac{a_0 b_0 - \omega b_0^2 - \sqrt{\omega^2 b_0^4 - 4\omega^2 b_{-1} b_0^2}}{b_0^2} \exp\left(\omega x^{\alpha} + m y^{\beta} + k z^{\gamma} - \omega^3 t^{\gamma} + \xi_0\right) + a_0 \\ + \left(\omega b_{-1} + \frac{a_0 b_{-1}}{b_0} - \frac{b_{-1}\sqrt{-\omega^2 b_0^2 (4b_{-1} - b_0^2)}}{b_0^2}\right) \exp\left(-\omega x - m y - k z + \omega^3 t - \xi_0\right) \end{array}\right]}{\left[\begin{array}{c} \exp\left(\omega x + m y + k z - \omega^3 t + \xi_0\right) + b_0 \\ + b_{-1} \exp\left(-\omega x - m y - k z + \omega^3 t - \xi_0\right) \end{array}\right]} \tag{27}$$

where a_0, b_0, b_{-1} and ω are free parameters. The performance of the solution $\psi_3(x, y, z, t)$ is presented in Figure 3 for $m = 1$, $k = 1$, $\xi_0 = 0$.

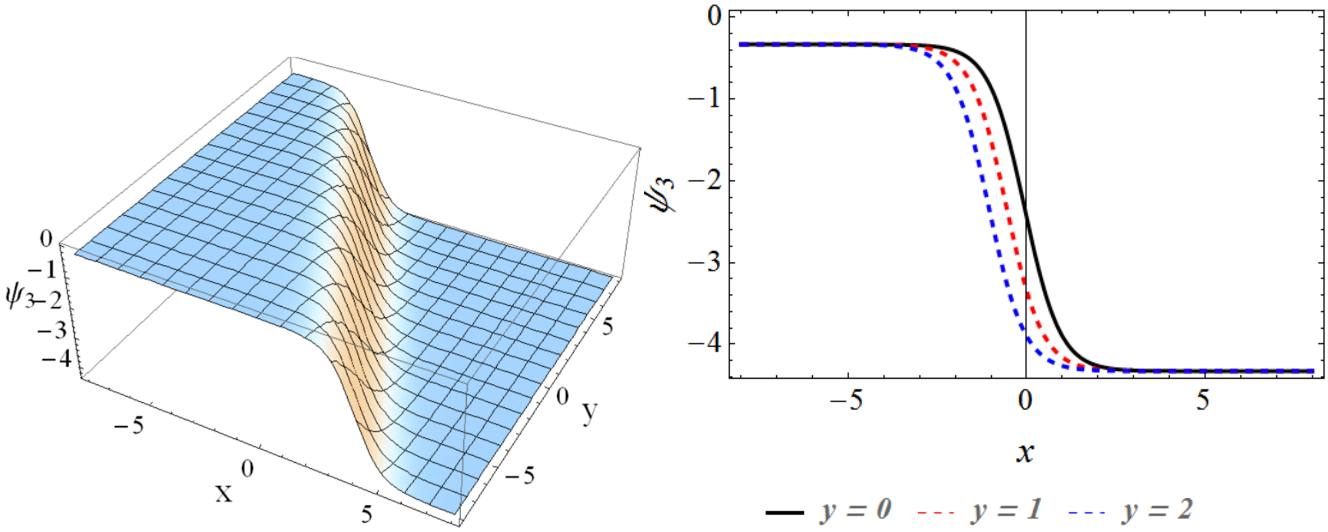

Figure 3. The 3D plot and 2D curve of the solution $\psi_3(x, y, z, t)$ for $\omega = 1$, $a_0 = 1$, $b_0 = 2$, $b_{-1} = -1$ when $z = 1$, $t = 0$.

Set 4: $a_1 = \frac{a_0 b_0 - \omega b_0^2 + \sqrt{\omega^2 b_0^4 - 4\omega^2 b_{-1} b_0^2}}{b_0^2}$, $a_0 = a_0$, $a_{-1} = \omega b_{-1} + \frac{a_0 b_{-1}}{b_0} + \frac{b_{-1}\sqrt{-\omega^2 b_0^2 (4b_{-1} - b_0^2)}}{b_0^2}$, $b_0 = b_0$, $b_{-1} = b_{-1}$, $v = -\omega^3$, $\omega = \omega$.

Then, we can obtain the fourth exact traveling wave solution (bright-dark wave solution) as:

$$\psi_4(x, y, t, z) = \frac{\left[\begin{array}{c} \frac{a_0 b_0 - \omega b_0^2 + \sqrt{\omega^2 b_0^4 - 4\omega^2 b_{-1} b_0^2}}{b_0^2} \exp\left(\omega x + m y + k z - \omega^3 t + \xi_0\right) + a_0 \\ + \left(\omega b_{-1} + \frac{a_0 b_{-1}}{b_0} + \frac{b_{-1}\sqrt{-\omega^2 b_0^2 (4b_{-1} - b_0^2)}}{b_0^2}\right) \exp\left(-\omega x - m y - k z + \omega^3 t - \xi_0\right) \end{array}\right]}{\left[\begin{array}{c} \exp\left(\omega x + m y + k z - \omega^3 t + \xi_0\right) + b_0 \\ + b_{-1} \exp\left(-\omega x - m y - k z + \omega^3 t - \xi_0\right) \end{array}\right]} \tag{28}$$

where a_0, b_0, b_{-1} and ω are free parameters. We plot the behavior of the solution $\psi_4(x, y, z, t)$ in Figure 4 with $m = 1$, $k = 1$, $\xi_0 = 0$.

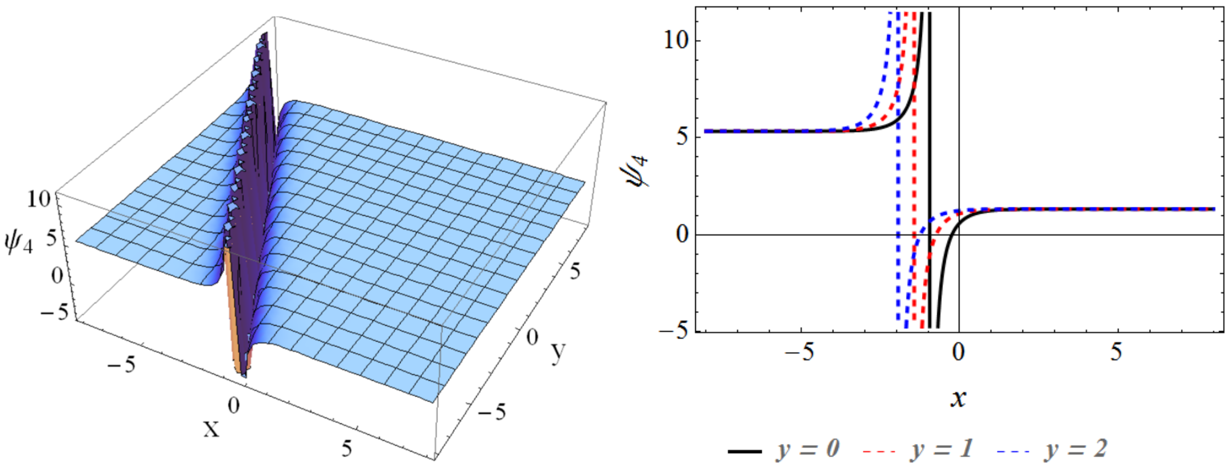

Figure 4. The 3D plot and 2D curve of the solution $\psi_4(x,y,z,t)$ for $\omega = 1, a_0 = 1, b_0 = 2, b_{-1} = -1$ when $z = 1, t = 0$.

Family 3

Set 5: $a_1 = \frac{a_{-1}-2\omega b_{-1}}{b_{-1}}$, $a_0 = \frac{a_{-1}b_{-1}b_0-\omega b^2_{-1}b_0-\sqrt{\omega^2 b^4_{-1}b^2_{-1}-4\omega^2 b^5_{-1}}}{b^2_{-1}}$, $a_{-1} = a_{-1}$, $b_0 = b_0$, $b_{-1} = b_{-1}$, $v = -\omega^3$, $\omega = \omega$.

Next, we can get the fifth exact traveling wave solution (kinky bright-dark solitary wave solution Form 1) as:

$$\psi_5(x,y,t,z) = \frac{\left[\begin{array}{c} \left(\frac{a_{-1}-2\omega b_{-1}}{b_{-1}}\right)\exp\left(\omega x + my + kz - \omega^3 t + \xi_0\right) + \frac{a_{-1}b_{-1}b_0-\omega b^2_{-1}b_0-\sqrt{\omega^2 b^4_{-1}b^2_{-1}-4\omega^2 b^5_{-1}}}{b^2_{-1}} \\ +a_{-1}\exp\left(-\omega x - my - kz + \omega^3 t - \xi_0\right) \end{array}\right]}{\left[\begin{array}{c} \exp\left(\omega x + my + kz - \omega^3 t + \xi_0\right) + b_0 \\ +b_{-1}\exp\left(-\omega x - my - kz + \omega^3 t - \xi_0\right) \end{array}\right]} \quad (29)$$

Here, the a_{-1}, b_0, b_{-1} and ω are free parameters. The solution $\psi_5(x,y,z,t)$ is presented in Figure 5 by using $m = 1, k = 1, \xi_0 = 0$.

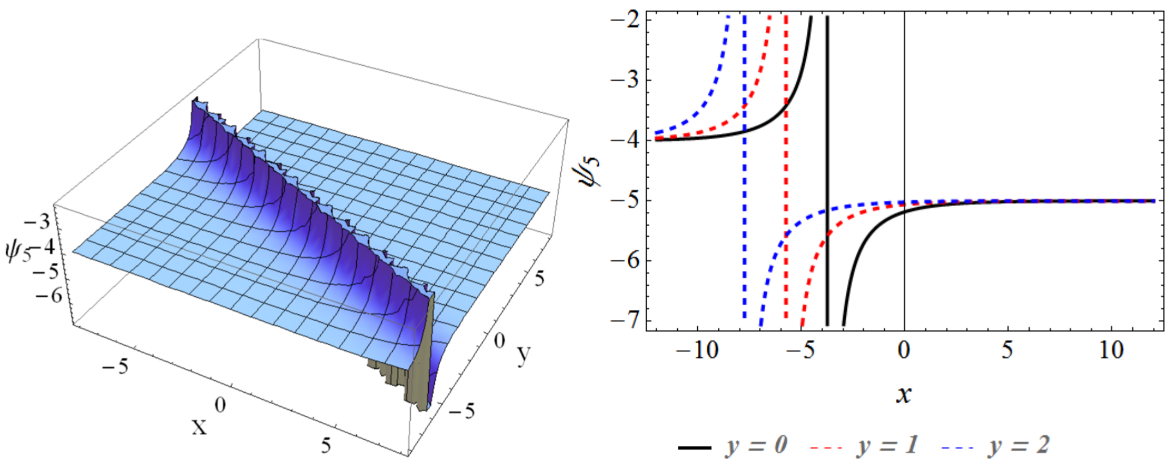

Figure 5. The 3D plot and 2D curve of the solution $\psi_5(x,y,z,t)$ for $\omega = 0.5, a_{-1} = 2, b_0 = 1, b_{-1} = -1$ when $z = 1, t = 1$.

Set 6: , $a_0 = \frac{a_{-1}b_{-1}b_0-\omega b^2_{-1}b_0+\sqrt{\omega^2 b^4_{-1}b^2_{-1}-4\omega^2 b^5_{-1}}}{b^2_{-1}}$, $a_{-1} = a_{-1}$, $b_0 = b_0$, $b_{-1} = b_{-1}$, $v = -\omega^3$, $\omega = \omega$.

Finally, we can get the sixth exact traveling wave solution (bright-dark wave solution) as

$$\psi_6(x,y,t,z) = \frac{\left[\begin{array}{c}\left(\frac{a_{-1}-2\omega b_{-1}}{b_{-1}}\right)\exp\left(\omega x+my+kz-\omega^3 t+\xi_0\right)+\frac{a_{-1}b_{-1}b_0-\omega b_{-1}^2 b_0+\sqrt{\omega^2 b_{-1}^4 b_{-1}^2-4\omega^2 b_{-1}^5}}{b_{-1}^2}\\ +a_{-1}\exp\left(-\omega x-my-kz+\omega^3 t-\xi_0\right)\end{array}\right]}{\left[\begin{array}{c}\exp\left(\omega x+my+kz-\omega^3 t+\xi_0\right)+b_0\\ +b_{-1}\exp\left(-\omega x-my-kz+\omega^3 t-\xi_0\right)\end{array}\right]} \tag{30}$$

where a_{-1}, b_0, b_{-1} and ω are free parameters. In this case, the contour of solution $\psi_6(x,y,z,t)$ is illustrated in Figure 6 by selecting $m=1$, $k=1$, $\xi_0=0$.

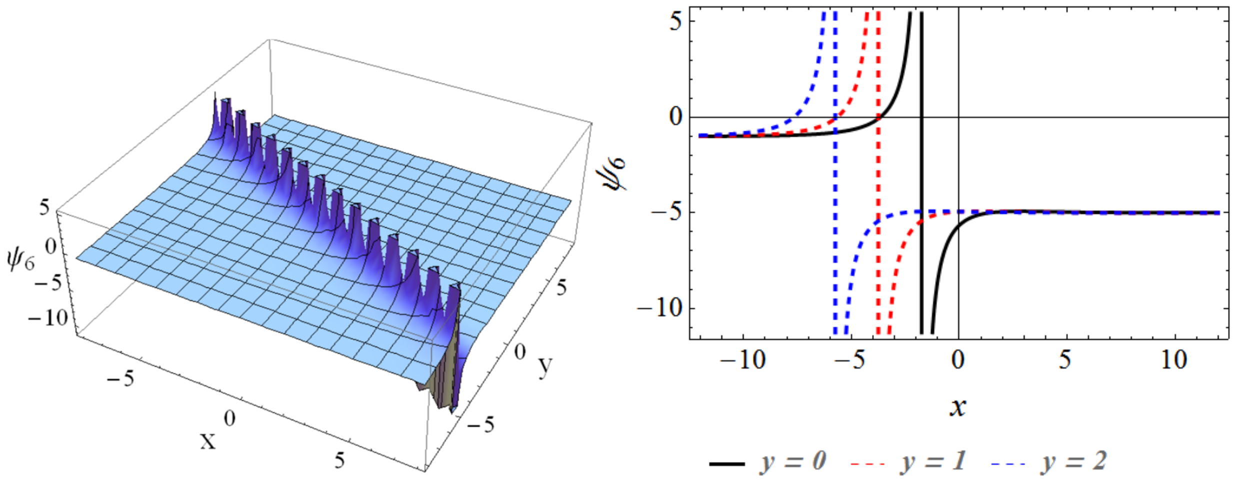

Figure 6. The 3D plot and 2D curve of the solution $\psi_6(x,y,z,t)$ for $\omega=0.5$, $a_{-1}=2$, $b_0=1$, $b_{-1}=-1$ when $z=1$, $t=1$.

3.2. Application of the HFF

In the view of Equation (12), we cannot solve it directly by the HFF. Here, we can make a transformation as:

$$\Im = \psi' \tag{31}$$

So Equation (12) becomes:

$$\omega^3\Im'' - 3\omega^2\Im^2 + v\Im = 0 \tag{32}$$

Which is

$$\Im'' - \frac{3}{\omega}\Im^2 + \frac{v}{\omega^3}\Im = 0 \tag{33}$$

From which, we obtain

$$f(\Im) = -\frac{3}{\omega}\Im^2 + \frac{v}{\omega^3}\Im \tag{34}$$

The periodic solution of Equation (32) is supposed with the form as:

$$\Im(\xi) = \Lambda\cos(\Omega\xi),\ \Omega > 0 \tag{35}$$

Based on the HFF, the amplitude frequency relationship can be easily determined as:

$$\Omega^2 = \left.\frac{df(\Im)}{d\Im}\right|_{\Im=\frac{\Lambda}{2}} = \frac{1}{\omega}\left(\frac{v}{\omega^2} - 3\Lambda\right) \tag{36}$$

With this, the periodic solution of Equation (32) can be obtained as:

$$\Im(\xi) = \Lambda \cos\left(\sqrt{\frac{1}{\omega}\left(\frac{v}{\omega^2} - 3\Lambda\right)}\xi\right) \tag{37}$$

In the view of Equation (31), we obtain:

$$\psi(\xi) = \frac{\Lambda}{\sqrt{\frac{1}{\omega}\left(\frac{v}{\omega^2} - 3\Lambda\right)}} \sin\left(\sqrt{\frac{1}{\omega}\left(\frac{v}{\omega^2} - 3\Lambda\right)}\xi\right) \tag{38}$$

Thus, the periodic wave solution of Equation (1) can be obtained as:
Set 7:

$$\psi_7(x, y, z, t) = \frac{\Lambda}{\sqrt{\frac{1}{\omega}\left(\frac{v}{\omega^2} - 3\Lambda\right)}} \sin\left[\sqrt{\frac{1}{\omega}\left(\frac{v}{\omega^2} - 3\Lambda\right)}(\omega x + my + kz + vt + \xi_0)\right] \tag{39}$$

By using $\Lambda = 1$, $\omega = \frac{1}{2}$, $m = \frac{1}{2}$, $k = 1$, $v = 1$, $\xi_0 = 0$, the performances of Equation (39) are described in Figure 7.

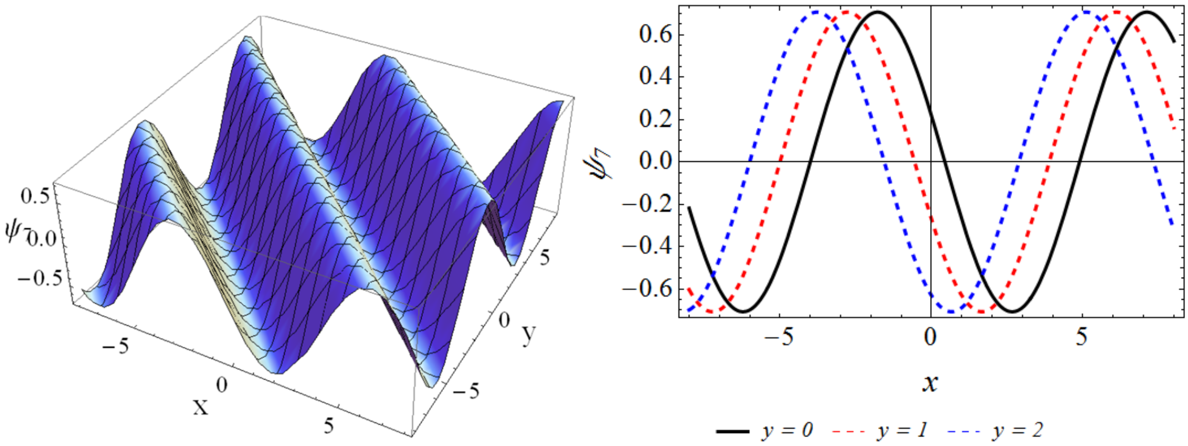

Figure 7. The 3D plot and 2D curve of the solution $\psi_7(x, y, z, t)$ when $z = 1$, $t = 1$.

4. Physical Explanation

This section provides the physical explanation of the results in Section 3. Figure 1 describes the contours of the solution $\psi_1(x, y, z, t)$ in the region $-8 \leq x \leq 8$, $-8 \leq y \leq 8$ for $z = 1$, $t = 1$. It can be seen that the wave is the dark-solitary wave. The behaviors of $\psi_2(x, y, z, t)$ are presented in Figure 2 through the three-dimensional contour and two-dimensional curve, where we can discover that the wave contour is the bright-dark wave. Figure 3 depicts the solution of $\psi_3(x, y, z, t)$ in the domain $-8 \leq x \leq 8$, $-8 \leq y \leq 8$ at $z = 1$, $t = 0$. By comparing Figure 3 with Figure 1, Figure 3 is similar with Figure 1, which is also the dark-solitary wave. We describe the performances of $\psi_4(x, y, z, t)$ in Figure 4 for $z = 1$, $t = 0$ in the interval $-8 \leq x \leq 8$, $-8 \leq y \leq 8$, which is the bright-dark wave in Figure 2. Figures 5 and 6 illustrate the solutions $\psi_5(x, y, z, t)$ and $\psi_6(x, y, z, t)$, respectively. By comparing them with Figures 2 and 4, we find that although Figures 5 and 6 are somewhat similar to Figures 2 and 4, they are still the bright-dark solitary wave. The behaviors of the solution $\psi_7(x, y, z, t)$ are plotted in Figure 7. It can be observed that the wave contour is a perfect periodic wave.

5. Conclusions and Future Recommendation

The (3+1)-dimensional BLMP equation that describes the incompressible fluid is investigated in this study. Two effective techniques, namely the EFM and HFF, are successfully applied to construct the abundant traveling wave solutions. Seven sets of the traveling wave solutions like the bright-dark wave, dark wave and periodic wave solutions are obtained. As we've seen from [14–22], the results disclosed in this work are all new, which can extend the study of the exact solutions of the (3+1)-dimensional BLMP equation. Finally, the solutions are all illustrated through the three-dimensional contours and two-dimensional curves. The results show that the proposed methods are concise and effective, which, in turn, are expected to be helpful for the study of nonlinear equations arising in physics.

Fractal and Fractional calculus has seen many advancements over the past years, and we have found that many classical models in current physics are being analyzed via this calculus [33–39]. Applying the Fractal and Fractional calculus to Equation (1) and extracting the exact solutions are the focus of future research.

Author Contributions: Conceptualization, K.-J.W.; methodology, K.-J.W.; writing—original draft preparation, K.-J.W.; supervision, K.-J.W.; writing—review and editing, Y.-N.C.; data curation, Y.-N.C. All authors have read and agreed to the published version of the manuscript.

Funding: This work is supported by the Key Programs of Universities in Henan Province of China (22A140006), Program of Henan Polytechnic University (B2018-40), the Innovative Scientists and Technicians Team of Henan Provincial High Education (21IRTSTHN016).

Data Availability Statement: The data that support the findings of this study are available from the corresponding author upon reasonable request.

Conflicts of Interest: This work does not have any conflict of interest.

Notation and Abbreviations

PDEs	partial differential equations
EFM	Exp-function method
HFF	He's frequency formulation
BLMP	Boiti–Leon–Manna–Pempinelli

References

1. Akram, G.; Sarfraz, M. Multiple optical soliton solutions for CGL equation with Kerr law nonlinearity via extended modified auxiliary equation mapping method. *Optik* **2021**, *242*, 167258. [CrossRef]
2. Cheemaa, N.; Seadawy, A.R.; Chen, S. More general families of exact solitary wave solutions of the nonlinear Schrödinger equation with their applications in nonlinear optics. *Eur. Phys. J. Plus* **2018**, *133*, 547. [CrossRef]
3. Wang, K.J.; Liu, J.H. Diverse optical solitons to the nonlinear Schrödinger equation via two novel techniques. *Eur. Phys. J. Plus* **2023**, *138*, 74. [CrossRef]
4. Wang, K.J.; Si, J.; Wang, G.D.; Shi, F. A new fractal modified Benjamin-Bona-Mahony equation: Its generalized variational principle and abundant exact solutions. *Fractals* **2023**. [CrossRef]
5. Arshad, M.; Seadawy, A.; Lu, D.; Wang, J. Travelling wave solutions of generalized coupled Zakharov–Kuznetsov and dispersive long wave equations. *Results Phys.* **2016**, *6*, 1136–1145. [CrossRef]
6. Soliman, A.A. The modified extended direct algebraic method for solving nonlinear partial differential equations. *Int. J. Nonlinear Sci.* **2008**, *6*, 136–144.
7. Asjad, M.I.; Munawar, N.; Muhammad, T.; Hamoud, A.A.; Emadifar, H.; Hamasalh, F.K.; Azizi, H.; Khademi, M. Traveling wave solutions to the Boussinesq equation via Sardar sub-equation technique. *AIMS Math.* **2022**, *7*, 11134–11149.
8. Onder, I.; Secer, A.; Ozisik, M.; Bayram, M. On the optical soliton solutions of Kundu-Mukherjee-Naskar equation via two different analytical methods. *Optik* **2022**, *257*, 168761. [CrossRef]
9. Wang, K.J. Diverse wave structures to the modified Benjamin-Bona-Mahony equation in the optical illusions field. *Mod. Phys. Lett. B* **2023**, *37*, 2350012. [CrossRef]
10. Wang, K.-J.; Shi, F.; Wang, G.-D. Abundant soliton structures to the (2+1)-dimensional Heisenberg ferromagnetic spin chain dynamical model. *Adv. Math. Phys.* **2023**, *2023*, 4348758. [CrossRef]
11. Yildirim, Y. Optical solitons of Biswas-Arshed equation by trial equation technique. *Optik* **2019**, *182*, 876–883. [CrossRef]

12. Ekici, M.; Sonmezoglu, A.; Biswas, A.; Belic, M.R. Optical solitons in (2+1)-Dimensions with Kundu-Mukherjee-Naskar equation by extended trial function scheme. *Chin. J. Phys.* **2019**, *57*, 72–77. [CrossRef]
13. Özkan, Y.S.; Yaşar, E.; Seadawy, A.R. On the multi-waves, interaction and Peregrine-like rational solutions of perturbed Radhakrishnan–Kundu–Lakshmanan equation. *Phys. Scr.* **2020**, *95*, 085205. [CrossRef]
14. Duan, X.; Lu, J. The exact solutions for the (3+1)-dimensional Boiti-Leon-Manna-Pempinelli equation. *Results Phys.* **2021**, *21*, 103820. [CrossRef]
15. Yel, G.; Aktürk, T. A new approach to (3+ 1) dimensional Boiti–Leon–Manna–Pempinelli equation. *Appl. Math. Nonlinear Sci.* **2020**, *5*, 309–316. [CrossRef]
16. Kaplan, M. Two different systematic techniques to find analytical solutions of the (2+1)-dimensional Boiti-Leon-Manna-Pempinelli equation. *Chin. J. Phys.* **2018**, *56*, 2523–2530. [CrossRef]
17. Ali, M.R.; Ma, W.X. New exact solutions of nonlinear (3+1)-dimensional Boiti-Leon-Manna-Pempinelli equation. *Adv. Math. Phys.* **2019**, *2019*, 9801638. [CrossRef]
18. Tang, Y.; Zai, W. New periodic-wave solutions for (2+1)- and (3+1)-dimensional Boiti–Leon–Manna–Pempinelli equations. *Nonlinear Dyn.* **2015**, *81*, 249–255. [CrossRef]
19. Liu, J.G. Double-periodic soliton solutions for the (3+1)-dimensional Boiti–Leon–Manna–Pempinelli equation in incompressible fluid. *Comput. Math. Appl.* **2018**, *75*, 3604–3613. [CrossRef]
20. Ali, K.K.; Mehanna, M.S. On some new soliton solutions of (3+1)-dimensional Boiti–Leon–Manna–Pempinelli equation using two different methods. *Arab. J. Basic Appl. Sci.* **2021**, *28*, 234–243. [CrossRef]
21. Najafi, M.N.S.A.M. New exact solutions to the integrable (2+1) and (3+1)-dimensional Boiti-Leon-Manna-Pempinelli equations. *Chin. Phys. C* **2013**, *37*, 010201.
22. Alenezi, A.M. Lump solutions of nonlinear (3+1)-dimensional for nonlinear partial differential equations. *Partial. Differ. Equ. Appl. Math.* **2020**, *2*, 100008. [CrossRef]
23. He, J.H.; Wu, X.H. Exp-function method for nonlinear wave equations. *Chaos Solitons Fractals* **2006**, *30*, 700–708. [CrossRef]
24. Zulfiqar, A.; Ahmad, J. Soliton solutions of fractional modified unstable Schrödinger equation using Exp-function method. *Results Phys.* **2020**, *19*, 103476. [CrossRef]
25. Wu, X.H.B.; He, J.H. Exp-function method and its application to nonlinear equations. *Chaos Solitons Fractals* **2008**, *38*, 903–910.
26. Ellahi, R.; Mohyud-Din, S.T.; Khan, U. Exact traveling wave solutions of fractional order Boussinesq-like equations by applying Exp-function method. *Results Phys.* **2018**, *8*, 114–120.
27. Wu, X.H.B.; He, J.H. Solitary solutions, periodic solutions and compacton-like solutions using the Exp-function method. *Comput. Math. Appl.* **2007**, *54*, 966–986. [CrossRef]
28. He, J.H. The simplest approach to nonlinear oscillators. *Results Phys.* **2019**, *15*, 102546. [CrossRef]
29. He, J.H. The simpler, the better: Analytical methods for nonlinear oscillators and fractional oscillators. *J. Low Freq. Noise Vib. Act. Control.* **2019**, *38*, 1252–1260. [CrossRef]
30. Alyousef, H.A.; Salas, A.H.; Alharthi, M.R.; El-Tantawy, S.A. Galerkin method, ansatz method, and He's frequency formulation for modeling the forced damped parametric driven pendulum oscillators. *J. Low Freq. Noise Vib. Act. Control.* **2022**, *41*, 1426–1445. [CrossRef]
31. He, J.H. Variational principle and periodic solution of the Kundu–Mukherjee–Naskar equation. *Results Phys.* **2020**, *17*, 103031. [CrossRef]
32. Wang, K.; Si, J. Dynamic properties of the attachment oscillator arising in the nanophysics. *Open Phys.* **2023**, *21*, 20220214. [CrossRef]
33. İlhan, E.; Kıymaz, İ.O. A generalization of truncated M-fractional derivative and applications to fractional differential equations. *Appl. Math. Nonlinear Sci.* **2020**, *5*, 171–188. [CrossRef]
34. Wang, K.L. Exact travelling wave solution for the fractal Riemann wave model arising in ocean science. *Fractals* **2022**, *30*, 2250143. [CrossRef]
35. Singh, J. Analysis of fractional blood alcohol model with composite fractional derivative. *Chaos Solitons Fractals* **2020**, *140*, 110127. [CrossRef]
36. Wang, K.-J.; Shi, F.; Si, J.; Liu, J.-H.; Wang, G.-D. Non-differentiable exact solutions of the local fractional Zakharov-Kuznetsov equation on the Cantor sets. *Fractals* **2023**, *31*, 2350028. [CrossRef]
37. He, J.H.; Ji, F.Y. Two-scale mathematics and fractional calculus for thermodynamics. *Therm. Sci.* **2019**, *23*, 2131–2133. [CrossRef]
38. Wang, K.J.; Liu, J.H.; Si, J.; Shi, F.; Wang, G.-D. N-soliton, breather, lump solutions and diverse travelling wave solutions of the fractional (2+1)-dimensional Boussinesq equation. *Fractals* **2023**, *31*, 2350023. [CrossRef]
39. He, C.H.; Liu, C.; He, J.H.; Gepreel, K.A. Low frequency property of a fractal vibration model for a concrete beam. *Fractals* **2021**, *29*, 2150117. [CrossRef]